UNCERTAINTY QUANTIFICATION IN THE ASSESSMENT OF PROGRESSIVE DAMAGE IN A SEVEN-STORY FULL-SCALE BUILDING SLICE

Ellen Simoen [1] , Babak Moaveni [2] , Joel P. Conte, Member, ASCE [3] and Geert Lombaert [4]

ABSTRACT

In this paper, Bayesian linear finite element (FE) model updating is applied for uncertainty quantification (UQ) in the vibration-based damage assessment of a seven-story reinforced concrete building slice. This structure was built and tested at full scale on the USCD-NEES shake table: progressive damage was induced by subjecting it to a set of historical earthquake ground motion records of increasing intensity. At each damage stage, modal characteristics such as natural frequencies and mode shapes were identified through low amplitude vibration testing; these data are used in the Bayesian FE model updating scheme. In order to analyze the results of the Bayesian scheme and gain insight into the information contained in the data, a comprehensive uncertainty and resolution analysis is proposed and applied to the seven-story building test case. It is shown that the Bayesian UQ approach and subsequent resolution analysis are effective in assessing uncertainty in FE model updating. Furthermore, it is demonstrated that the Bayesian FE model updating approach provides insight into the regularization of its often ill-posed deterministic counterpart.

Keywords: vibration-based damage assessment, structural health monitoring, uncertainty quantification, FE model updating, regularization, Bayesian inference, resolution analysis

INTRODUCTION

[1]PhD Student, KU Leuven, Department of Civil Engineering, Kasteelpark Arenberg 40 box 2448, B-3001 Leuven, Belgium. Email: ellen.simoen@bwk.kuleuven.be

[2]Assis. Prof., Tufts University, Department of Civil and Environmental Engineering, 200 College Avenue, Medford, MA 02155, USA. Email: babak.moaveni@tufts.edu

[3]Prof., University of California at San Diego, Department of Structural Engineering, 9500 Gilman Drive, La Jolla, CA 92093-0085, USA. Email: jpconte@ucsd.edu

[4]Assoc. Prof., KU Leuven, Department of Civil Engineering, Kasteelpark Arenberg 40 box 2448, B-3001 Leuven, Belgium. Email: geert.lombaert@bwk.kuleuven.be

In structural engineering, it is common practice to use finite element (FE) models for design, analysis, and assessment of civil structures. For existing structures, FE model updating techniques provide a tool for calibrating FE models based on observed structural response (Mottershead and Friswell 1993; Friswell and Mottershead 1995). Structural FE model updating most often makes use of vibration data, i.e. response time histories obtained from forced (Heylen et al. 1997), ambient (Peeters and De Roeck 2001) or combined (Reynders and De Roeck 2008) vibration testing, as well as modal characteristics (e.g., natural frequencies and mode shapes) extracted from these vibration tests. FE model updating is frequently applied for structural damage assessment, where damage is located and quantified in a non-destructive manner (Teughels et al. 2002). Localized damage in a structure results in a local reduction of stiffness; therefore the updating parameters typically represent the effective stiffness of a number of substructures. The FE model updating process involves determining the optimal values of a set of FE model parameters by solving an inverse problem, where the objective is to minimize the discrepancy between FE model predictions and measured modal data. However, the inverse problem is typically ill-posed (due to e.g., low data resolution, over-parameterization, non-linearities,…), which means that accounting for measurement and modeling errors or uncertainties is crucial when applying FE model updating techniques.

One possible approach to incorporate uncertainty regarding the observations and the model predictions into the FE model updating process is to adopt a probabilistic scheme based on Bayesian inference (Box and Tiao 1973; Beck and Katafygiotis 1998; Jaynes 2003). This approach makes use of probability theory to model uncertainty; the plausibility or degree of belief attributed to the values of uncertain parameters is represented by specifying probability density functions (PDFs) for the uncertain parameters. A prior (marginal or joint) PDF reflects the prior knowledge about the parameter(s), i.e., the knowledge before any observations are made. Using Bayes' theorem, the prior PDF is transformed into a posterior PDF, accounting both for uncertainty in the prior information as well as for uncertainty in the experimental data and FE model predictions. This transformation is performed through the so-called likelihood function, which reflects how well the

FE model can explain the observed data and which can be computed using the probabilistic model of the prediction error.

The Bayesian inference approach has gained interest amongst uncertainty quantification methods in recent years, mostly because of its firm foundation on probability theory and its rigorous treatment of uncertainties. The method has a wide range of application domains; in a civil engineering context, topics include geophysics (Mosegaard and Tarantola 1995; Schevenels et al. 2008) and structural dynamics, where it is applied for e.g. reliability studies and structural health monitoring (SHM) (Beck and Au 2002; Sibilio et al. 2007; Sohn and Law 1997; Vanik et al. 2000; Yuen and Katafygiotis 2002), model class selection (Beck and Yuen 2004; Muto and Beck 2008; Yuen 2010b) and optimal sensor placement (Papadimitriou et al. 2000; Yuen et al. 2001).

One of the advantages of the Bayesian model updating method is that it is firmly set in a probabilistic framework, which means that a well established set of tools exists to investigate the posterior results. The analysis of the posterior PDF is often referred to as resolution analysis, and typically consists of the computation of standard posterior statistics such as mean values, modes, standard deviations and covariances, which yield insight into how well individual parameters are resolved from the data, and whether statistical correlations exist between them. An additional eigenvalue analysis based on the prior and posterior covariance matrices helps identify well-resolved features or parameter combinations (Tarantola 2005). A useful link to information entropy (Papadimitriou et al. 2000; Papadimitriou 2004) allows for further insight into the relative resolution of different parameter combinations.

The Bayesian FE model updating approach furthermore shows the distinct advantage that it can be easily related to its deterministic counterpart. As the likelihood function provides a measure for the discrepancy between the FE model predictions and the measured/identified data, minimizing this function (with respect to the model parameters) corresponds to solving the deterministic inverse problem referred to above. It is shown in this paper that by including the prior PDF into this minimization scheme, a regularization term is introduced naturally into the (often ill-posed) deterministic optimization problem, without having to revert to standard regularization methods that require additional decision-making and may appear heuristic.

In this paper, the Bayesian UQ technique will be used for uncertainty quantification in the vibration-based damage assessment of a seven-story reinforced concrete building slice (Panagiotou et al. 2011). This test structure was built and tested at full scale on the UCSD-NEES shake table, and therefore yields a unique set of controlled experimental data, representing a realistic mid-rise building subject to earthquake excitation. Progressive damage was induced in the structure, allowing for deterministic damage assessment at several stages through linear FE model updating, as performed in (Moaveni et al. 2010). In these deterministic updating schemes and associated sensitivity analyses (Moaveni et al. 2007; Moaveni et al. 2009; Moaveni et al. 2011), it became apparent that this problem is subject to many uncertainties (regarding e.g. the measured modal data and the FE model) that have large influence on the results of the damage identification scheme. This indicates the ill-posedness of the inverse problem at hand, and the necessity to assess the effect of these sources of uncertainty on the FE model updating results in a comprehensive manner.

The paper starts by introducing the seven-story test case in the next section. The subsequent section establishes the framework and methodology of the Bayesian inference scheme for vibration-based linear FE model updating, and elaborates the Bayesian multi-stage damage assessment procedure for the seven-story test structure. A following section continues with the description of the resolution analysis used to investigate the damage assessment results obtained from the Bayesian inference schemes. Results and conclusions are discussed in a final section.

THE SEVEN-STORY TEST STRUCTURE

The seven-story test structure (Moaveni et al. 2007; Moaveni et al. 2009; Moaveni et al. 2010; Moaveni et al. 2011), representing a slice of a prototype reinforced concrete mid-rise residential building, was built and tested at full-scale on the UCSD-NEES shake table (Figure 1a). The structure consists of two perpendicular walls (i.e. a main wall and a back wall for transverse stability), seven concrete floor slabs, an auxiliary post-tensioned column for torsional stability, and four gravity columns to transfer the weight of the slabs to the ground level (Figure 1b).

A progressive damage pattern was induced in the test structure through four historical earthquake records, leading to 5 damage states S0 to S4 (Table 1). After each seismic excitation sequence, ambient vibration tests and low-amplitude white-noise base excitation tests were performed in order to obtain modal characteristics of the structure; the experimentally identified natural frequencies and damping ratios of the first three longitudinal modes are listed in Table 2 for each damage state. The natural frequencies evidently decrease as the damage increases; the damping ratios show no particular trend, most likely due to the fact that damping ratios generally cannot be measured with sufficient accuracy to allow for any statement regarding their values (Reynders et al. 2008). Figure 2 shows the corresponding employed mode shapes obtained at damage state S0 using 28 sensors located along the main wall and on the floor slabs. Note that for the damage identification, only the mode shape measurements obtained using 14 sensors located along the main wall are employed. In the following, experimental eigenvalues and mode shapes are denoted as $\tilde{\lambda}_r = (2\pi f_{\mathrm{exp},r})^2$ and $\tilde{\boldsymbol{\phi}}_r \in \mathbb{R}^{N_o}$, respectively, where N_o represents the number of observed degrees of freedom. Both experimental data are collected in the vector $\tilde{\mathbf{d}} = \{\ldots, \tilde{\lambda}_r, \ldots, \tilde{\boldsymbol{\phi}}_r^{\mathrm{T}}, \ldots\}^{\mathrm{T}}$.

These modal data are used in five consecutive damage analyses: for each damage state, Bayesian FE model updating is applied to quantify the uncertainties on the damage identification results. To this end, a detailed 3D linear elastic FE model was constructed with 322 shell and truss elements and $N_d = 2418$ degrees of freedom (Figure 3a), using the general-purpose FE analysis program FEDEASLab (Filippou and Constantinides 2004). In order to model the damage, the structure is divided into 10 substructures, each consisting of part of the main wall (Figure 3b). It is assumed that each substructure has a uniform effective stiffness (Young's modulus); these stiffness values will be the updating parameters $\boldsymbol{\theta}_{\mathrm{M}}$ in the Bayesian updating schemes (see below). The stiffness values are *effective* stiffness values in the sense that they represent not only the true stiffness of a particular substructure, but are also affected by other elements that are not included in the parameterization (e.g. characteristics of the floor slabs or flange wall). Initial values $\boldsymbol{\theta}_{\mathrm{M}}^{\mathrm{init}}$ of the 10 Young's moduli are obtained trough concrete cylinder testing at various heights along the building (Moaveni et al. 2010); these values will be used to represent the initial FE model in the updating schemes:

$$\boldsymbol{\theta}_{\mathrm{M}}^{\mathrm{init}} = \left[\begin{array}{cccccccccc} 24.5 & 24.5 & 26.0 & 26.0 & 34.8 & 34.8 & 30.2 & 28.9 & 32.1 & 33.5 \end{array}\right]^{\mathrm{T}} \quad \mathrm{GPa} \tag{1}$$

The FE model allows for the computation of the modal data as a function of the model parameters $\boldsymbol{\theta}_{\mathrm{M}}$, where the modal data consist of N_m eigenvalues λ_r and corresponding mode shapes $\boldsymbol{\phi}_r \in \mathbb{R}^{N_d}$, which are the solutions of the (undamped) eigenvalue equation $\mathbf{K}(\boldsymbol{\theta}_{\mathrm{M}})\boldsymbol{\Phi} = \mathbf{M}\boldsymbol{\Phi}\boldsymbol{\Lambda}$, where $\mathbf{K}(\boldsymbol{\theta}_{\mathrm{M}})$ is the FE model stiffness matrix and $\mathbf{M}$ the mass matrix. $\boldsymbol{\Phi}$ collects the eigenvectors $\boldsymbol{\phi}_r$ corresponding to the eigenvalues λ_r located on the diagonal of $\boldsymbol{\Lambda}$. In the Bayesian updating scheme, these computed modes are paired to the experimentally identified modes by means of the Modal Assurance Criterion (or MAC); furthermore, a least squares scaling factor is introduced in order to ensure that paired modes are scaled equally. The set of computed data for a certain model parameter set $\boldsymbol{\theta}_{\mathrm{M}}$ is referred to as $\mathbf{G}_{\mathrm{M}}(\boldsymbol{\theta}_{\mathrm{M}})$ in the following.

BAYESIAN FE MODEL UPDATING

The basic concept of Bayesian inference is that evidence (usually in the form of experimental observations) is used to update or re-infer the probability that a certain hypothesis is true. Important to note here is that Bayesian methods use the Bayesian interpretation of probability, which differs from the frequentist interpretation of probability. In the frequentist interpretation, probability is seen as a relative frequency of a certain event, whereas in the Bayesian interpretation, probability reflects the relative plausibility or degree of belief attributed to a certain event or proposition (here: a model in a model class), given the available information. In this interpretation – often termed the Cox-Jaynes interpretation (Jaynes 2003; Cox 1946) – probability can be seen as an extended logic, i.e. as an extension of a Boolean logic to a multi-valued logic for plausible inference.

The next subsections present the Bayesian updating methodology used here, starting with some preliminary specifications of the basic framework concerning model classes and uncertainties.

Models and model classes

In general terms, a model $\mathcal{M}_{\mathrm{M}}(\boldsymbol{\theta}_{\mathrm{M}})$ belonging to the model class $\mathcal{M}_{\mathrm{M}}$ provides a map from the parameters $\boldsymbol{\theta}_{\mathrm{M}}$ to an output vector $\mathbf{d}$ through the transfer operator $\mathbf{G}_{\mathrm{M}}$:

$$\mathcal{M}_{\mathrm{M}}(\boldsymbol{\theta}_{\mathrm{M}}): \quad \mathbf{G}_{\mathrm{M}}(\boldsymbol{\theta}_{\mathrm{M}}) = \mathbf{d} \tag{2}$$

In the ideal case, the model output $\mathbf{G}_{\mathrm{M}}(\boldsymbol{\theta}_{\mathrm{M}})$ corresponds perfectly to the true system output $\mathbf{d}$. This is the main starting point for deterministic model updating or parameter identification, where the objective is to determine the model parameters $\boldsymbol{\theta}_{\mathrm{M}}$ for a given set of observed system outputs $\mathbf{d}$. However, Eq. (2) is only valid when it is assumed that the underlying fundamental physics of the system are fully known. This is of course never the case, as no model is capable of perfectly representing the behavior of the true physical system. A modeling error $\boldsymbol{\eta}_{\mathrm{G}}$ is therefore always present, and can be described as the discrepancy between the model predictions $\mathbf{G}_{\mathrm{M}}(\boldsymbol{\theta}_{\mathrm{M}})$ and the true system output $\mathbf{d}$, i.e. $\boldsymbol{\eta}_{\mathrm{G}} = \mathbf{G}_{\mathrm{M}}(\boldsymbol{\theta}_{\mathrm{M}}) - \mathbf{d}$. In general, two forms of modeling error are distinguished: (1) *model structure errors*, caused for example by incorrect assumptions on the governing physical equations of the system (e.g. linearity instead of non-linearity) or by an insufficient model order, and (2) *model parameter errors*, caused by e.g. inaccurate geometric and material properties.

As the true system output has to be measured and processed experimentally, the data $\mathbf{d}$ are always subject to measurement error. This error can be an aleatory random measurement or estimation error, or can be a bias error caused by imperfections in the measurement equipment or the subsequent signal processing. This causes an additional source of discrepancy between the observed structure behavior $\tilde{\mathbf{d}}$ and the real structure response $\mathbf{d}$; this difference is defined as the measurement error $\boldsymbol{\eta}_{\mathrm{D}} = \mathbf{d} - \tilde{\mathbf{d}}$. Eliminating the unknown true system output $\mathbf{d}$ from the error equations and collecting both errors on the right hand side of the resulting equation yields:

$$\mathbf{G}_{\mathrm{M}}(\boldsymbol{\theta}_{\mathrm{M}}) - \tilde{\mathbf{d}} = \boldsymbol{\eta}_{\mathrm{G}} + \boldsymbol{\eta}_{\mathrm{D}} = \boldsymbol{\eta} \tag{3}$$

The sum of both errors is equal to the total observed prediction error $\boldsymbol{\eta}$, defined as the difference between the observed and predicted response quantities. This also implies that, when no information is available on the errors, there is no way to distinguish between measurement and modeling errors, as only the total observed prediction error can be identified. The above expressions serve as a starting point for the Bayesian uncertainty quantification method.

Bayesian inference methodology

The general principle behind Bayesian model updating is that the structural model parameters $\boldsymbol{\theta}_{\mathrm{M}} \in \mathbb{R}^{N_M}$ that parametrize model class $\mathcal{M}_{\mathrm{M}}$ are modeled as random variables, i.e. probability density functions (PDFs) are assigned to these parameters, which are then updated in the inference scheme based on the available information. Measurement and modeling uncertainty are taken into account by modeling the respective errors as random variables as well: PDFs are assigned to $\boldsymbol{\eta}_{\mathrm{G}}$ and $\boldsymbol{\eta}_{\mathrm{D}}$, which are parametrized by parameters $\boldsymbol{\theta}_{\mathrm{G}} \in \mathbb{R}^{N_G}$ and $\boldsymbol{\theta}_{\mathrm{D}} \in \mathbb{R}^{N_D}$. These parameters are added to the structural model parameters $\boldsymbol{\theta}_{\mathrm{M}}$ to form the general model parameter set $\boldsymbol{\theta} = \{\boldsymbol{\theta}_{\mathrm{M}}, \boldsymbol{\theta}_{\mathrm{G}}, \boldsymbol{\theta}_{\mathrm{D}}\}^{\mathrm{T}} \in \mathbb{R}^{N}$. This in fact corresponds to adding two probabilistic model classes to the structural model class $\mathcal{M}_{\mathrm{M}}$ to form a joint model class $\mathcal{M} = \mathcal{M}_{\mathrm{M}} \times \mathcal{M}_{\mathrm{G}} \times \mathcal{M}_{\mathrm{D}}$, parametrized by $\boldsymbol{\theta}$.

It has to be noted here that introducing a probabilistic model for the errors is only one of several possible approaches for stochastic modeling of the uncertainties (Soize 2011); alternatively, one could revert to non-parametric approaches (Soize 2000) acting directly on the operators of the model, e.g., making use of random matrix theory (Mehta 2004), or so-called *generalized* probabilistic approaches (Soize 2010) that combine parametric and non-parametric approaches.

To express the updated joint PDF of the unknown parameters $\boldsymbol{\theta}$, given some observations $\tilde{\mathbf{d}}$ and a certain joint model class $\mathcal{M}$, Bayes' theorem is used:

$$p(\boldsymbol{\theta} \mid \tilde{\mathbf{d}}, \mathcal{M}) = c\, p(\tilde{\mathbf{d}} \mid \boldsymbol{\theta}, \mathcal{M})\, p(\boldsymbol{\theta} \mid \mathcal{M}) \tag{4}$$

where $p(\boldsymbol{\theta}|\tilde{\mathbf{d}}, \mathcal{M})$ is the updated or posterior joint PDF of the model parameters given the measured data $\tilde{\mathbf{d}}$ and the assumed model class $\mathcal{M}$; c is a normalizing constant (independent of $\boldsymbol{\theta}$) that ensures that the posterior PDF integrates to one; $p(\tilde{\mathbf{d}}|\boldsymbol{\theta},\mathcal{M})$ is the PDF of the observed data given the parameters $\boldsymbol{\theta}$; and $p(\boldsymbol{\theta}|\mathcal{M})$ is the initial or prior joint PDF of the parameters. In the following, the explicit dependence on the model class $\mathcal{M}$ is omitted in order to simplify the notations.

Prior PDF

The prior PDF $p(\boldsymbol{\theta})$ represents the probability distribution of the model parameters $\boldsymbol{\theta}$ in the absence of observations or measurement results. In most cases, this PDF is chosen based on engineering judgment and the available prior information; alternatively, the Principle of Maximum Entropy (Jaynes 1957) provides an objective method to determine suitable prior PDFs that yield maximum uncertainty given the available information.

Likelihood function

The PDF of the experimental data $p(\tilde{\mathbf{d}}|\boldsymbol{\theta})$ can be interpreted as a measure of how good a model succeeds in explaining the observations $\tilde{\mathbf{d}}$. As this PDF also represents the likelihood of observing the data $\tilde{\mathbf{d}}$ when the model is parameterized by $\boldsymbol{\theta}$, it is also referred to as the *likelihood* function $L(\boldsymbol{\theta}|\tilde{\mathbf{d}})$. It reflects the contribution of the measured data $\tilde{\mathbf{d}}$ in the determination of the updated PDF of the model parameters $\boldsymbol{\theta}$, and may be determined according to the Total Probability Theorem and Eq. (3) using the probabilistic models of the measurement and modeling errors:

$$L(\boldsymbol{\theta} \mid \tilde{\mathbf{d}}) \equiv p(\tilde{\mathbf{d}} \mid \boldsymbol{\theta}) = \int p(\mathbf{d} \mid \boldsymbol{\theta})\, p(\tilde{\mathbf{d}} \mid \boldsymbol{\theta}, \mathbf{d})\, d\mathbf{d} \tag{5}$$

$$= \int p_{\boldsymbol{\eta}_{\mathrm{D}}}(\mathbf{d} - \tilde{\mathbf{d}}; \boldsymbol{\theta}_{\mathrm{D}})\, p_{\boldsymbol{\eta}_{\mathrm{G}}}(\mathbf{G}_{\mathrm{M}}(\boldsymbol{\theta}_{\mathrm{M}}) - \mathbf{d}; \boldsymbol{\theta}_{\mathrm{G}})\ d\mathbf{d} \tag{6}$$

where $p_{\boldsymbol{\eta}_{\mathrm{D}}}(\mathbf{d} - \tilde{\mathbf{d}}; \boldsymbol{\theta}_{\mathrm{D}})$ corresponds to the probability of obtaining a measurement error $\boldsymbol{\eta}_{\mathrm{D}}$, given the PDF of $\boldsymbol{\eta}_{\mathrm{D}}$ parameterized by $\boldsymbol{\theta}_{\mathrm{D}}$, and where $p_{\boldsymbol{\eta}_{\mathrm{G}}}(\mathbf{G}_{\mathrm{M}}(\boldsymbol{\theta}_{\mathrm{M}}) - \mathbf{d}; \boldsymbol{\theta}_{\mathrm{G}})$ represents the probability of obtaining a modeling error $\boldsymbol{\eta}_{\mathrm{G}}$ when the PDF of $\boldsymbol{\eta}_{\mathrm{G}}$ is known and parameterized by $\boldsymbol{\theta}_{\mathrm{G}}$. Here, it is implicitly assumed that the modeling error and measurement error are statistically independent variables.

The above equations show that the likelihood function can be computed as the convolution of the PDFs of the measurement and modeling error. When no information is available on the individual errors, as is most often the case, the likelihood function can be constructed using the probabilistic model of the total prediction error $\boldsymbol{\eta}$ ($= \mathbf{G}_{\mathrm{M}}(\boldsymbol{\theta}_{\mathrm{M}}) - \tilde{\mathbf{d}}$), parameterized by $\boldsymbol{\theta}_{\eta}$:

$$L(\boldsymbol{\theta} \mid \tilde{\mathbf{d}}) \equiv p(\tilde{\mathbf{d}} \mid \boldsymbol{\theta}) = p(\boldsymbol{\eta}; \boldsymbol{\theta}_{\eta}) \tag{7}$$

Prediction error model

In some cases, a realistic estimate can be made concerning the probabilistic model representing the prediction error, for instance based on the analysis of measurement results (Reynders et al. 2008) or when information is available on the specific nature of the modeling and/or measurement error. In most practical applications, however, very little or no information is at hand regarding the characteristics of these errors. Then, it can be opted to make a reasonable assumption regarding the model class, and include the parameters of the probabilistic error model in the Bayesian scheme; additionally, several candidate model classes can be compared using Bayesian model class selection (Beck and Yuen 2004).

Alternatively, assumptions can be made regarding both the total prediction error model class and the corresponding parameters, which means the parameter set in the Bayesian scheme reduces to $\boldsymbol{\theta} = \{\boldsymbol{\theta}_{\mathrm{M}}\} \in \mathbb{R}^{N_\theta}$. Often, a zero-mean Gaussian prediction error characterized by a covariance matrix $\boldsymbol{\Sigma}_{\eta}$ is adopted, which means the likelihood function in Eq. (7) simplifies to a multivariate normal PDF :

$$L(\boldsymbol{\theta} \mid \tilde{\mathbf{d}}) \propto \exp\left[-\frac{1}{2}\boldsymbol{\eta}^{\mathrm{T}}\boldsymbol{\Sigma}_{\eta}^{-1}\boldsymbol{\eta}\right] \tag{8}$$

Maximum likelihood estimate

Maximizing, for example, the Gaussian (log) likelihood function in Eq. (8) is equivalent to solving the following optimization problem:

$$\hat{\boldsymbol{\theta}}^{\mathrm{ML}} = \arg\min_{\boldsymbol{\theta}} \left\{\frac{1}{2}\boldsymbol{\eta}^{\mathrm{T}}\boldsymbol{\Sigma}_{\eta}^{-1}\boldsymbol{\eta}\right\} \tag{9}$$

where $\hat{\boldsymbol{\theta}}^{\mathrm{ML}}$ is the so-called Maximum Likelihood or ML estimate of the parameter set $\boldsymbol{\theta}$. For an uncorrelated prediction error, i.e. a diagonal covariance matrix $\Sigma_{\boldsymbol{\eta}}$, the optimization problem in equation (9) corresponds to a weighted least squares optimization problem, while for a correlated prediction error it corresponds to a generalized least squares problem.

Solving a least squares problem as stated in Eq. (9) in fact corresponds to solving a classical deterministic FE model updating problem, as the objective function aims to minimize the discrepancy between model predictions and measured data. Note that the weights given to the discrepancies are inversely proportionate to the appointed error variances, which corresponds to giving more weight to more accurate data.

Posterior PDF

When the prior PDF and likelihood function are determined, Eq. (4) allows for the updating of the joint PDF of the model parameters $\boldsymbol{\theta}$ based on experimental observations of the system. For most practical applications where multiple parameters are involved, computing the posterior joint and marginal PDFs requires solving high-dimensional integrals. Therefore use is often made of asymptotic expressions (Beck and Katafygiotis 1998; Papadimitriou et al. 1997) or sampling methods such as Markov Chain Monte Carlo (MCMC) methods (Gamerman 1997) and its derivatives, e.g. Delayed-Rejection Adaptive Metropolis-Hastings MCMC (Haario et al. 2001; Haario et al. 2006) and Transitional MCMC (Ching and Chen 2007).

Link between prior PDF and regularization An interesting feature of the Bayesian scheme is that it provides a very natural way to regularize the ill-posed optimization problem described above. As mentioned above, maximizing the likelihood function corresponds to solving the unregularized least squares problem. By maximizing the posterior PDF (in order to find the Maximum A Posteriori or MAP estimate $\hat{\boldsymbol{\theta}}^{\mathrm{MAP}}$), the prior PDF is included into this scheme, naturally introducing a regularization term into the corresponding deterministic optimization problem. For example, adopting a Gaussian likelihood function leads to the following expression for the MAP estimate:

$$\hat{\boldsymbol{\theta}}^{\mathrm{MAP}} = \arg\min_{\boldsymbol{\theta}} \{J_{\mathrm{MAP}}\} = \arg\min_{\boldsymbol{\theta}} \left\{ \frac{1}{2}\boldsymbol{\eta}^{\mathrm{T}}\boldsymbol{\Sigma}_{\boldsymbol{\eta}}^{-1}\boldsymbol{\eta} - \log p(\boldsymbol{\theta}) \right\} \tag{10}$$

The second term in this equation corresponds to a Tikhonov-type regularization term, based on the prior information available. This clearly shows that the deterministic counterpart of the Bayesian inference scheme incorporates regularization in a natural way, without having to revert to re-parameterization or other standard regularization methods. Moreover, information contained in the prior PDF (e.g., positivity of the parameters) is automatically enforced in the deterministic optimization scheme. This will be illustrated below for the seven-story test structure.

Bayesian FE model updating of the seven-story test structure

To quantify the uncertainties in the multi-stage damage assessment of the seven-story building slice introduced above, the Bayesian inference method elaborated above is applied to this test case. As mentioned above, the employed structural response here consists of a number of modal characteristics identified from vibration data obtained at several damage states. The Bayesian updating scheme is performed for each of the considered damage states, starting with the undamaged state S0 in a first preliminary updating stage, where the initial values $\boldsymbol{\theta}^{\mathrm{init}}$ in Eq. (1) are adopted as most probable prior point or Maximum A Priori (MAPr) estimate of the model parameters $\boldsymbol{\theta}$.

For each of the next stages S1 to S4, it is proposed to adopt the Maximum A Posteriori (MAP) estimate of the model parameters obtained in the previous stage as MAPr estimate of the current stage. This is in accordance with the progressive damage pattern that was induced in the structure: in each stage Sk, only data obtained in that particular damage state are used to compute the posterior PDF of $\boldsymbol{\theta}$, but as the structure was already damaged in the previous stage S$(k-1)$, it is plausible to adopt the MAP parameter values of the previous damage state as the maximum prior values of the current state. The posterior PDF of a stage Sk is not chosen as prior PDF for the next stage S$(k+1)$, as this would imply that data set Sk provides information on the structure in the damage state S$(k+1)$. Therefore, the peak values of the posterior PDF are used to construct the prior PDF of the following damage stage, but the shape of the prior PDFs is kept the same over all damage states. Note that in this way, it is also avoided that very narrow PDFs are chosen for the prior PDFs, which could lead to biased results in the updating scheme. The general Bayesian updating scheme is summarized as follows:

S0: The prior PDF $p(\boldsymbol{\theta}; \boldsymbol{\theta}^{\text{init}})$ of the model parameters $\boldsymbol{\theta}$, parameterized by the fixed set $\boldsymbol{\theta}^{\text{init}}$, is updated to a posterior PDF $p(\boldsymbol{\theta}|\tilde{\mathbf{d}}^{(S0)})$ through the likelihood function $L(\boldsymbol{\theta}|\tilde{\mathbf{d}}^{(S0)})$, which is constructed using the measured modal data $\tilde{\mathbf{d}}^{(S0)}$ obtained in damage state S0:

$$p(\boldsymbol{\theta} \mid \tilde{\mathbf{d}}^{(S0)}) \propto p(\boldsymbol{\theta}; \boldsymbol{\theta}^{\text{init}})\, L(\boldsymbol{\theta} \mid \tilde{\mathbf{d}}^{(S0)}) \tag{11}$$

S1: In the next stage S1, the MAP estimate $\hat{\boldsymbol{\theta}}_{\text{MAP}}^{(S0)}$ obtained in S0 is adopted as maximum a priori estimate in the prior PDF of S1 (see below). To obtain the posterior PDF for this stage, the prior has to be multiplied with the likelihood function $L(\boldsymbol{\theta} \mid \tilde{\mathbf{d}}^{(S1)})$ which is constructed using modal data obtained in S1:

$$p(\boldsymbol{\theta} \mid \tilde{\mathbf{d}}^{(S1)}) \propto p(\boldsymbol{\theta}; \hat{\boldsymbol{\theta}}_{\text{MAP}}^{(S0)})\, L(\boldsymbol{\theta} \mid \tilde{\mathbf{d}}^{(S1)}) \tag{12}$$

Sk: This scheme is repeated for the next stages, such that for an arbitrary stage Sk the following updating equation is obtained:

$$p(\boldsymbol{\theta} \mid \tilde{\mathbf{d}}^{(Sk)}) \propto p(\boldsymbol{\theta}; \hat{\boldsymbol{\theta}}_{\text{MAP}}^{(S(k-1))})\, L(\boldsymbol{\theta} \mid \tilde{\mathbf{d}}^{(Sk)}) \tag{13}$$

In the next subsections, it is discussed how the prior PDFs and likelihood functions are determined for each damage state.

Prior PDF

The joint prior PDF for the model parameters $\boldsymbol{\theta}$ is determined based on the Maximum Entropy Principle (Soize 2008). For multivariate cases, the Maximum Entropy principle always leads to independent prior variables, which means the joint prior PDF is constructed as the product of the marginal prior PDFs. In order to determine suitable prior PDFs for the individual parameters, the available prior information has to be evaluated; a priori, it is known that the stiffness parameters have a positive support, and a given mean value μ_j. Furthermore, in order to ensure that the response attains finite variance, θ_j and $1/\theta_j$ should be second order variables. It can be shown that given this prior information, the Maximum Entropy principle yields a Gamma-distribution (Soize 2003), which leads to the following expression of the joint prior PDF for the first undamaged stage S0:

$$p(\boldsymbol{\theta};\boldsymbol{\theta}^{\text{init}}) = \prod_{j=1}^{N_\theta} p(\theta_j;\theta_j^{\text{init}}) = \prod_{j=1}^{N_\theta} \frac{\theta_j^{\alpha_j-1}}{\beta_j^{\alpha_j}\Gamma(\alpha_j)} \exp\left(-\frac{\theta_j}{\beta_j}\right) \tag{14}$$

where shape factor α_j $(= \mu_j^2/\sigma_j^2 = 1/\text{COV}_j^2)$ and scale factor β_j $(= \mu_j/\alpha_j)$ depend on the values of μ_j and σ_j assigned to parameter θ_j. The shape factor α_j is only dependent on the corresponding coefficient of variation (COV_j). It is expected that damage will cause large deviations from these measured initial values in lower stories, but smaller deviations in higher stories; therefore, the following values of COV_j are proposed, for all damage states:

$$\text{COV}_j = \begin{cases} 0.35 & \text{for} \quad j = 1,\ldots,3 \\ 0.25 & \text{for} \quad j = 4,\ldots,10 \end{cases} \tag{15}$$

The scale factor β_j differs for each damage state, and will therefore be denoted as $\beta_j^{(Sk)}$ for a particular damage state Sk. For the first damage state S0, $\beta_j^{(S0)}$ is chosen such that the maximum a priori point (i.e., the mode of the prior PDF) corresponds to the initial value θ_j^{init}. This leads to the following expression for $\beta_j^{(S0)}$:

$$\beta_j^{(S0)} = \frac{\theta_j^{\text{init}}\,\text{COV}_j^2}{1-\text{COV}_j^2} \tag{16}$$

For a stage Sk (with $k > 0$), it is assumed that the MAP estimate $\hat{\boldsymbol{\theta}}_{\text{MAP}}^{(S(k-1))}$ of the previous damage stage S$(k-1)$ is used as most probable prior point of the current stage, which yields:

$$\beta_j^{(Sk)} = \frac{\hat{\theta}_{\text{MAP},j}^{(S(k-1))}\text{COV}_j^2}{1-\text{COV}_j^2} \tag{17}$$

In Figure 4a, a contour plot is given of the marginal prior PDFs at S0; in Figure 4b, the marginal prior PDF at S0 is shown for substructure 1, with a MAPr value equal to $\theta_1^{\mathrm{init}} = 24.5$ GPa (see Eq. (1)).

Likelihood function

For each damage stage, an uncorrelated zero-mean Gaussian prediction error is adopted:

$$\boldsymbol{\eta}^{(Sk)} \sim \mathcal{N}(\mathbf{0}, \boldsymbol{\Sigma}_{\boldsymbol{\eta}}^{(Sk)}) \tag{18}$$

where it is assumed that the covariance matrix $\boldsymbol{\Sigma}_{\boldsymbol{\eta}}^{(Sk)}$ is known. As mentioned above, error parameters could be included in the Bayesian scheme in an effort to estimate the total prediction error model (or the individual contributions of measurement and modeling error), but due to the relatively low data resolution it is opted here to simply assume a fixed prediction error model. In this test case, the prediction error $\boldsymbol{\eta}^{(Sk)}$ represents the discrepancy between measured and computed eigenvalues and mode shapes:

$$\boldsymbol{\eta}^{(Sk)} = \begin{bmatrix} \boldsymbol{\eta}_{\lambda}^{(Sk)} \\ \boldsymbol{\eta}_{\phi}^{(Sk)} \end{bmatrix} = \left[\ldots, \eta_{\lambda,r}^{(Sk)}, \ldots, \eta_{\phi,r,\ell}^{(Sk)}, \ldots\right]^{\mathrm{T}} \tag{19}$$

where $r = 1, \ldots, N_m$ and $\ell = 1, \ldots, N_o$. The assumption of a zero mean value for $\boldsymbol{\eta}^{(Sk)}$ corresponds to assuming that the computed values will on average be equal to the measured values. In order to construct the covariance matrices $\boldsymbol{\Sigma}_{\boldsymbol{\eta}}^{(Sk)}$, standard deviations are proposed for the eigenvalue and mode shape discrepancies. For the eigenvalues discrepancies $\eta_{\lambda,r}^{(Sk)}$, it is assumed that the standard deviations are proportionate to the measured values:

$$\eta_{\lambda,r}^{(Sk)} \sim \mathcal{N}\left(0, c_{\lambda,r}^2 (\tilde{\lambda}_r^{(Sk)})^2\right) \tag{20}$$

In this way, the values of $c_{\lambda,r}$ can be interpreted as appointed coefficients of variation. For the mode shape components, a slightly different strategy is adopted in order to avoid assigning extremely small standard deviations to components with measured values close to zero. Instead, for each mode shape component ℓ of a mode r, the same standard deviation is assumed proportionate to the norm of mode shape r, such that:

$$\eta_{\phi,r,\ell}^{(Sk)} \sim \mathcal{N}\left(0, c_{\phi,r}^2 \parallel \tilde{\boldsymbol{\phi}}_r^{(Sk)} \parallel^2\right) \tag{21}$$

The values of $c_{\lambda,r}$ and $c_{\phi,r}$ reflect the magnitude of the combined modeling and measurement error. In this particular case, however, only limited information is available regarding the measurement error, in the form of observed variabilities of identified natural frequencies using different system identification methods and ambient vibration tests (Moaveni et al. 2011; Moaveni et al. 2012).

Based on these studies and engineering judgment, the following values for $c_{\lambda,r}$ and $c_{\phi,r}$ are proposed for the three experimentally identified modes, for all damage states:

$$\mathbf{c}_\lambda = \mathbf{c}_\phi = \left[\begin{array}{ccc} 0.069 & 0.150 & 0.100 \end{array}\right] \tag{22}$$

Using the expressions in Eqs. (8), (20) and (21), the likelihood function for a single data set $\tilde{\mathbf{d}}^{(Sk)}$ can now be written as:

$$L(\boldsymbol{\theta} \mid \tilde{\mathbf{d}}^{(Sk)}) \propto \exp\left[-\frac{1}{2}(\boldsymbol{\eta}^{(Sk)})^{\mathrm{T}}(\boldsymbol{\Sigma}_{\boldsymbol{\eta}}^{(Sk)})^{-1}(\boldsymbol{\eta}^{(Sk)})\right] = \exp\left[-\frac{1}{2}J_{\mathrm{ML}}(\boldsymbol{\theta}, \tilde{\mathbf{d}}^{(Sk)})\right] \tag{23}$$

where $J_{\mathrm{ML}}(\boldsymbol{\theta}, \tilde{\mathbf{d}}^{(Sk)})$ is the ML objective function (often also referred to as the *misfit* function):

$$J_{\mathrm{ML}}(\boldsymbol{\theta}, \tilde{\mathbf{d}}^{(Sk)}) = \sum_{r=1}^{N_m} \frac{1}{c_{\lambda,r}^2} \frac{(\lambda_r(\boldsymbol{\theta}) - \tilde{\lambda}_r^{(Sk)})^2}{(\tilde{\lambda}_r^{(Sk)})^2} + \sum_{r=1}^{N_m} \frac{1}{c_{\phi,r}^2} \frac{\parallel \boldsymbol{\phi}_r(\boldsymbol{\theta}) - \tilde{\boldsymbol{\phi}}_r^{(Sk)} \parallel^2}{\parallel \tilde{\boldsymbol{\phi}}_r^{(Sk)} \parallel^2} \tag{24}$$

MAP estimate and deterministic updating

As mentioned above, the MAP objective function defined in Eq. (10) can be adopted to obtain a deterministic objective function that incorporates all available information, and allows for automatic regularization based on the prior information. For the seven-story test structure, the MAP objective function for a damage state Sk is constructed according to Eq. (10) as:

$$J_{\mathrm{MAP}}(\boldsymbol{\theta}, \tilde{\mathrm{d}}^{(Sk)}) = \frac{1}{2}(\boldsymbol{\eta}^{(Sk)})^{\mathrm{T}}(\boldsymbol{\Sigma}_{\boldsymbol{\eta}}^{(Sk)})^{-1}(\boldsymbol{\eta}^{(Sk)}) - \log p(\boldsymbol{\theta}; \hat{\boldsymbol{\theta}}_{\mathrm{MAP}}^{(S(k-1))}) = \frac{1}{2}J_{\mathrm{ML}}(\boldsymbol{\theta}, \tilde{\mathrm{d}}^{(Sk)}) + J_{\mathrm{MAPr}}^{(Sk)} \tag{25}$$

The first term in this objective function corresponds to the standard least squares objective function elaborated above, and it can be easily verified that the second term acts as a regularization term. Elaborating $J_{\mathrm{MAPr}}^{(Sk)}$ for the seven-story structure yields (up to a constant term):

$$J_{\mathrm{MAPr}}^{(Sk)} = \sum_{j=1}^{N_\theta}\left(\frac{\theta_j}{\beta_j^{(Sk)}} + (1-\alpha_j)\log\theta_j\right) \tag{26}$$

It is clear that the first term in the above equation corresponds to a weighted L1 regularization term, which encourages sparsity of the parameter vector such that only the most relevant parameters remain. The second term acts as a barrier function which enforces the constraint of positivity on the model parameters $\boldsymbol{\theta}$, as the factor $(1-\alpha_j)$ is here always negative and the corresponding second term therefore pushes the solution for θ_j away from zero in the positive direction. This clearly illustrates that the term $J_{\mathrm{MAPr}}^{(Sk)}$ (or $-\log p(\boldsymbol{\theta})$ in general) can be interpreted as a regularization term which is based only on the available prior information and avoids having to revert to other standard regularization approaches. Furthermore, constraints contained in the prior information are automatically enforced, which bypasses the need for explicit definition of constraints in the optimization scheme, simplifying the implementation substantially. Therefore, it can be stated that, especially in combination with the Maximum Entropy principle, this approach constitutes a general and rigorous way to determine a suitable objective function in deterministic FE model updating problems.

Note that the deterministic model updating results can be employed to validate the MAP results of the Bayesian scheme obtained through e.g. MCMC simulation. In this context, it is interesting to note that the Hessian of the objective function (evaluated in the optimum) can be shown to be an asymptotic approximation of the inverse posterior covariance matrix of the updating parameters

(Beck and Katafygiotis 1998; Papadimitriou et al. 1997). Since in many optimization algorithms, the Hessian is computed as a by-product in the optimization of the problem defined in Eq. (10), this provides an additional means of validating results or a way to perform an initial reconnaissance of the posterior updating results.

Results of the Bayesian updating scheme

For each damage stage, the joint posterior PDF of the model parameters $\boldsymbol{\theta}$ was sampled using the Adaptive Metropolis-Hastings MCMC method (Haario et al. 2001). Several convergence measures (i.e. running mean values, running standard deviations and running correlation between samples) showed that for all damage states, convergence was reached after 200 000 samples. The marginal posterior PDFs were obtained by kernel smoothing density estimation.

Results for damage state S0 The normalized marginal posterior PDFs for S0 are shown in Figure 5; Table 3 reports the corresponding MAP estimate, and the mean value, standard deviation and coefficient of variation for each of the marginal PDFs. Also found in this table are the MAP values as obtained through minimization of the MAP objective function defined in Eq. (25); the unconstrained optimization is performed in Matlab using a local gradient-based optimization algorithm through the standard Matlab routine `fminunc`.

Comparing the MAP estimates $\boldsymbol{\theta}_{\mathrm{opt}}^{\mathrm{MAP}}$ and $\boldsymbol{\theta}_{\mathrm{MCMC}}^{\mathrm{MAP}}$ as obtained through the deterministic optimization and the MCMC scheme, respectively, it is found that the values are very similar but not identical. Examination of the MAP residuals (i.e. $J_{\mathrm{MAP}}^{(S0)}$, $J_{\mathrm{ML}}^{(S0)}$ and $J_{\mathrm{MAPr}}^{(S0)}$ evaluated at the MAP estimates) confirms that both MAP estimates are in fact very close, exhibiting residuals differing by less than 0.1%, although the MAP estimate obtained from the deterministic updating routine always results in smaller residuals ($J_{\mathrm{MAP,opt}}^{(S0)} = -301.5$ and $J_{\mathrm{MAP,MCMC}}^{(S0)} = -301.2$). This difference is most likely explained by the fact that the estimates are obtained through algorithms with very different objectives. The gradient-based optimization routine is specifically designed to find the MAP estimate, whereas the sampling method randomly searches the whole parameter space and is therefore sometimes less effective and less accurate in finding the global optimum.

Furthermore, it is found that the MAP objective function in this case exhibits non-smooth behavior (most likely due to mode shape matching), which implies that the joint posterior PDF is most likely not peaked at a single point but rather exhibits many local maxima of similar probability, making this a locally identifiable case (Katafygiotis and Beck 1998; Yuen 2010a). This situation is commonly encountered in Bayesian updating applications, and here further explains the difference between the two obtained MAP estimates. In the following, only the MCMC results are discussed in further detail.

When examining the MAP-estimate and posterior mean values, it is clear that the effective stiffness in the undamaged state of the building was initially underestimated in most substructures, except for the bottom substructure 1, which shows a low value compared to the initial value θ_1^{init}. Furthermore, among all the stiffness parameters, this bottom substructure stiffness is best identified from the data and prior information, as the COV is reduced from 35% to about 24%. For the top seven substructures, the uncertainty is reduced only to a very limited extent below the prior COV of 25%: the posterior COV-values range from 23% to 24.8%. In Figure 6, the normalized prior and posterior marginal PDFs are compared for substructures 1 and 5, which immediately confirms these findings: the posterior PDF for the bottom substructure has become much narrower, whereas for substructure 5 the posterior PDF is practically the same as the prior PDF. It should be noted here that it is apparent that both posterior PDFs are not Gaussian, which implies that mean values, standard deviations and associated COV values should be interpreted with appropriate care.

Results for damage states S1 to S4 In Figures 7a–7d, contour plots of the posterior marginal PDFs of the effective stiffness parameters $\boldsymbol{\theta}_{\mathrm{M}}$ are shown for damage states S1 to S4. The MAP-estimates (obtained through MCMC) of the stiffness values are compared in Figure 8 for all damage states, the corresponding values are reported in Table 4, together with the posterior marginal coefficients of variation.

The MAP stiffness values generally reduce as the damage increases, especially the stiffness in the bottom substructures – where the actual damage from the shake table tests is concentrated.

The most drastic stiffness reduction occurs for substructure 1, where the MAP stiffness at S4 decreases to about 1 GPa due to the very high level of damage. For some substructures, sometimes a small increase in MAP stiffness is found for a higher damage state, which is most likely caused by insensitivity of the model predictions to changes in these parameter values, resulting in the identifiability issues discussed above. This is corroborated by the fact that the posterior uncertainty regarding these substructures remains largely the same over all damage states.

The significantly decreased stiffness value for substructure 7 in damage state S4 was also observed in the previously performed deterministic damage identification study (Moaveni et al. 2010), where it was determined to be a false alarm. Most likely the low stiffness value is explained by the fact that the updating parameters will also account for damage in other structural elements that are not included in the updating scheme, such as the floor slabs or the flange wall. Note also the increased stiffness values in adjacent substructure 8, which most likely compensate for the stiffness decrease observed in substructure 7.

Overall, the lower part of the structure (substructures 1–3) shows a larger COV reduction compared to the top substructures, especially in states S0 and S1, and particularly for the bottom substructure, where the posterior COV is even reduced to about half of the prior COV in S4. These observations are most likely explained by considering modal curvatures: firstly, the lower section of the structure is in any case subjected to higher modal curvatures, meaning the modal data are more sensitive to local stiffness changes and thus provide more information for the updating scheme in these areas. Moreover, structural damage results in an additional increase in modal curvature, explaining the substantial uncertainty reduction in the most damaged bottom substructure 1. This also implies that, as the damage increases, the data become relatively less informative regarding substructures with less extensive damage. Examining the posterior COV-values for higher damage levels S3 and S4 confirms this statement: for substructures 2–10 the uncertainty no longer reduces, and sometimes even increases slightly due to this effect.

All these findings indicate that the available data are not always as informative regarding the chosen model parameters. This also implies that the available prior information plays an important role in the results obtained through the Bayesian inference scheme. In order to confirm these statements and to obtain more insight into the underlying causes of these findings, a detailed resolution and uncertainty analysis may be carried out, as presented in the next section.

RESOLUTION ANALYSIS

The first step in a resolution analysis typically consists in determining quantities such as MAP estimates, posterior mean values and standard deviations, which yield basic insight into the resolution of the parameters. However, standard deviations do not provide information regarding possible correlations between parameters, therefore the prior and posterior covariance matrices, denoted as $\mathbf{S}_{\mathrm{pr}}$ and $\mathbf{S}_{\mathrm{po}}$ respectively, may be calculated to this end. Usually, the off-diagonal correlation values are most easily interpreted and compared by computing the prior and posterior correlation coefficient matrices.

To further investigate the resolution of (combinations of) the parameters, one could revert to Principal Component Analysis (PCA), where the correlated posterior variables are transformed to a set of mutually orthogonal (uncorrelated) variables by transforming the posterior data to a new orthogonal coordinate system. The coordinates of this new system are termed the principal components. The transformation is done in such a way that the first principal component corresponds to a direction in the parameter space that exhibits the largest variability in the posterior data; in other words, the principal components correspond to linear combinations of the original variables (or parameters) ranked according to decreasing posterior variance. The principal components correspond to the set of eigenvectors of the posterior covariance matrix $\mathbf{S}_{\mathrm{po}}$. The eigenvectors are ranked according to increasing associated eigenvalue, which corresponds to increasing posterior variance.

Although PCA is an interesting technique to investigate the posterior resolution of the parameters in the parameter space, it does not take into account any information contained in the prior information. This is why several authors (Tarantola 2005; Duijndam 1988) propose to examine instead the solution of the following extended eigenvalue problem:

$$\mathbf{S}_{\mathrm{po}}\mathbf{X} = \mathbf{\Lambda}\mathbf{S}_{\mathrm{pr}}\mathbf{X} \tag{27}$$

It can be shown that the eigenvectors in $\mathbf{X}$ correspond to mutually orthogonal directions in the parameter space ranked according to decreasing reduction from prior to posterior variance, when ranked according to increasing eigenvalue. Each eigenvalue gives a measure for the ratio of posterior to prior variance in the corresponding direction in the parameter space, which means that the eigenvector associated with the smallest eigenvalue corresponds to a direction in the parameter space that shows the largest reduction from prior to posterior variance. In other words, the values of the eigenvalues express the relative degree of the reduction from prior to posterior variance in the principal directions in the parameter space.

Relation to information entropy

The information entropy is often used as a measure of the resulting uncertainty in the Bayesian estimates of the model parameters (Papadimitriou et al. 2000). For the posterior PDF, it is defined as:

$$h(\boldsymbol{\theta}) = \mathbb{E}\left[-\log p(\boldsymbol{\theta}|\mathbf{d})\right] \tag{28}$$

Under certain asymptotic conditions (i.e. global identifiability (Katafygiotis and Beck 1998), or availability of a large amount of data compared to the prior information, such that the posterior PDF can be approximated by a Gaussian PDF around the ML or MAP point), the information entropy can be approximated as (Papadimitriou 2004):

$$h(\boldsymbol{\theta}) \approx \frac{1}{2}N\log(2\pi e) - \frac{1}{2}\log\left[\det\mathbf{Q}(\hat{\boldsymbol{\theta}}^{\mathrm{ML}})\right] \tag{29}$$

where $\mathbf{Q}$ denotes the Fisher Information Matrix (FIM), evaluated at the maximum likelihood point $\hat{\boldsymbol{\theta}}^{\mathrm{ML}}$. The FIM is equal to the negative of the Hessian of the log likelihood, and it can be shown that this Hessian is (approximately) equal to the negative inverse of the posterior covariance matrix

(Papadimitriou et al. 1997). This in fact corresponds to assuming that the posterior PDF can be asymptotically approximated by a Gaussian PDF centered at the MAP or ML point, with a posterior covariance matrix $\mathbf{S}_{\mathrm{po}}$, as the entropy expression in Eq. (29) can be reformulated as:

$$h(\boldsymbol{\theta}) \approx \frac{1}{2} \log \left[(2\pi e)^N \det \mathbf{S}_{\mathrm{po}} \right] \tag{30}$$

which can be recognized as the information entropy of a multivariate Gaussian PDF.

The entropy discrepancy Δh may be computed as a measure of the information that was gained from the observations. It is a non-negative scalar (as adding information always leads to decreasing entropy) which is defined as:

$$\Delta h = h_{\mathrm{pr}} - h_{\mathrm{po}} \tag{31}$$

Using the approximative entropy expression in Eq. (29), the following approximation for the entropy discrepancy is obtained:

$$\Delta h \approx -\frac{1}{2} \log \det \left(\mathbf{S}_{\mathrm{pr}}^{-1} \mathbf{S}_{\mathrm{po}} \right) = -\frac{1}{2} \sum_{k=1}^{N_\theta} \log \lambda_k \tag{32}$$

where λ_k are the eigenvalues of the eigenvalue problem defined in Eq. (27). This means that by computing the values $d_k = -\frac{1}{2} \log \lambda_k$ corresponding to the eigenvectors (or directions in the parameter space) $\mathbf{X}_k$, the relative contribution of the different directions to the total resolution can be quantified.

Resolution analysis for the seven-story test structure

The posterior correlation coefficient matrix for the substructure stiffnesses is shown in Figure 9a for damage state S0, from which it can be deduced that, in contrast to the prior situation, the model parameters are a posteriori no longer independent variables. However, the correlations between the model parameters generally remain very limited, except for the bottom substructures where correlation coefficients of -0.42 are attained. Note that the occurring correlations are mostly negative, which is to be expected as contrasting stiffnesses (i.e. high in one and low in the other) in (adjacent) substructures would explain the data almost equally well.

In Figure 9b, the first and last two (normalized) eigenvectors or parameter combinations are shown, corresponding to the best and worst resolved directions in the parameter space. It is clear that the best resolved parameter combination contains predominantly the first substructure stiffness, whereas the two worst resolved directions contain all seven of the top substructure stiffness values. This is in very good agreement with the previously discussed results. By examining the eigenvalues associated with these eigenvectors, their relative contributions to the total resolution can be quantified in terms of entropy reduction. In this case, the total entropy reduction Δh equals 1.21, of which a part of ($-1/2 \log \lambda_1 =$) 0.92 or 76% is contributed by reduction in the direction X_1. Directions X_9 and X_{10} together contribute a mere 0.04% to the total entropy reduction, which also confirms the results found above. Note that, even though the conditions for using the approximate entropy expressions may not be completely fulfilled for this particular case study, the entropy analysis yields important insights into the resolution of the different parameter combinations.

For damage states S1 to S3, very similar results are found. In Figure 10a, the posterior correlation coefficient matrix is shown for damage state S4, and in Figure 10b, the best and two worst resolved directions in the parameter space are displayed. The negative correlations between adjacent substructures 6–9 , and especially between substructures 7 and 8 ($\rho_{7,8} = -0.46$) are immediately apparent; substructure 7 even shows a negative correlation with all other substructures. This corresponds to the observations made above regarding the false alarm and compensation by substructure 8.

The eigenvector analysis confirms that the effective stiffness of substructure 1 is by far the best resolved feature, accounting for almost 80% of the entropy reduction through the data in damage state S4. Furthermore, the worst resolved parameter directions encompass almost all other substructures, especially substructures 6–8, indicating that very little information about these parameters can be obtained from the data used in this study. Therefore, large uncertainty remains associated with the false alarm detected in the previous analyses.

It is confirmed that the worst resolved features incorporate the top substructures 4–10 for all damage states, which indicates that the FE model of the seven-story test building is most likely over-parameterized, as the data appears to contain very little to no information regarding these top seven parameters.

CONCLUSIONS

In this paper, Bayesian linear FE model updating is used for uncertainty quantification in the assessment of progressive damage in a seven-story reinforced concrete building slice subjected to seismic tests on the USCSD-NEES shake table. To this end, experimentally identified modal data obtained in five different damage states are employed. In the Bayesian FE model updating approach, a zero-mean uncorrelated Gaussian prediction error is assumed, and to construct the prior PDFs, the Maximum A Posteriori (MAP) estimate of a certain damage state is adopted as the Maximum A Priori estimate of the next damage state. The posterior joint PDF of the substructure stiffness parameters is estimated using a MCMC approach and the MAP results are validated through a deterministic updating scheme based on the Bayesian approach. The results of the Bayesian FE model updating scheme are assessed further by performing a detailed resolution analysis, which allows for improved insight into which (and to what extent) characteristics of the damaged structure are resolved through the Bayesian scheme using the identified modal data. Furthermore, it is shown how the incorporation of prior information relates to the regularization of the corresponding deterministic FE model updating problem.

Overall, the Bayesian approach succeeded in identifying the damage in the seven-story structure and in quantifying the corresponding uncertainties at all damage states. It was found that the data contain little information concerning the top stories of the building, as the uncertainty on the stiffness parameters representing this area could not be reduced through the observed data. This was confirmed by a detailed resolution analysis, which showed that parameter combinations containing the upper seven substructures were always least resolved by the available data. However, the lower substructures, and the bottom substructure 1 in particular, are well resolved by the data, most likely due to the higher damage level and higher modal curvatures in these areas of the structure.

These findings lead to the conclusion that for this structure, damage can be detected (SHM Level 1 (Rytter 1993)) effectively, but that for the purpose of reducing the uncertainty regarding damage quantification and localization (SHM levels 2–3) in the upper stories, more elaborate experimental data are desirable. This can be accomplished by increasing the number of mode shapes and/or measurement DOFs, or by including other types of modal data such as modal strains.

REFERENCES

Beck, J. and Au, S.-K. (2002). "Bayesian updating of structural models and reliability using Markov Chain Monte Carlo simulation." *ASCE Journal of Engineering Mechanics*, 128(4), 380–391.

Beck, J. and Katafygiotis, L. (1998). "Updating models and their uncertainties. I: Bayesian statistical framework." *ASCE Journal of Engineering Mechanics*, 124(4), 455–461.

Beck, J. and Yuen, K.-V. (2004). "Model selection using response measurements: Bayesian probabilistic approach." *ASCE Journal of Engineering Mechanics*, 130(2), 192–203.

Box, G. and Tiao, G. (1973). *Bayesian inference in statistical analysis*. Addison-Wesley.

Ching, J. and Chen, Y.-C. (2007). "Transitional Markov Chain Monte Carlo method for Bayesian model updating, model class selection, and model averaging." *ASCE Journal of Engineering Mechanics*, 133(7), 816–832.

Cox, R. (1946). "Probability, frequency and reasonable expectation." *American Journal of Physics*, 14(1), 1–13.

Duijndam, A. (1988). "Bayesian estimation in seismic inversion. Part II: Uncertainty analysis." *Geophysical Prospecting*, 36(8), 899–918.

Filippou, F. and Constantinides, M. (2004). "Fedeaslab getting started guide and simulation examples." *Technical report NEESgrid-2004-22*, <http://fedeaslab.berkeley.edu>.

Friswell, M. and Mottershead, J. (1995). *Finite element model updating in structural dynamics*. Kluwer Academic Publishers, Dordrecht, The Netherlands.

Gamerman, D. (1997). *Markov Chain Monte Carlo: stochastic simulation for Bayesian inference*. Chapman & Hall, London.

Haario, H., Laine, M., Mira, A., and Saksman, E. (2006). "DRAM: Efficient adaptive MCMC." *Statistics and Computing*, 16(4), 339–354.

Haario, H., Saksman, E., and Tamminen, J. (2001). "An adaptive Metropolis algorithm." *Bernouilli*, 7(2), 223–242.

Heylen, W., Lammens, S., and Sas, P. (1997). *Modal analysis theory and testing*. Department of Mechanical Engineering, Katholieke Universiteit Leuven, Leuven, Belgium.

Jaynes, E. (1957). "Information theory and statistical mechanics." *The Physical Review*, 106(4), 620–630.

Jaynes, E. (2003). *Probability Theory. The Logic of Science*. Cambridge University Press, Cambridge, UK.

Katafygiotis, L. and Beck, J. (1998). "Updating models and their uncertainties. II: Model identifiability." *ASCE Journal of Engineering Mechanics*, 124(4), 463–467.

Mehta, M. (2004). *Random Matrices*. Elsevier, San Diego, CA, 3rd edition.

Moaveni, B., Barbosa, A., Conte, J., and Hemez, F. (2007). "Uncertainty analysis of modal parameters obtained from three system identification methods." *Proceedings of IMAC-XXV, International Conference on Modal Analysis*, Orlando, Florida, USA (February).

Moaveni, B., Conte, J., and Hemez, F. (2009). "Uncertainty and sensitivity analysis of damage identification results obtained using finite element model updating." *Computer-Aided Civil and Infrastructure Engineering*, 24(5), 320–334.

Moaveni, B., He, X., Conte, J., and Restrepo, J. (2010). "Damage identification study of a seven-story full-scale building slice tested on the UCSD-NEES shake table." *Structural Safety*, 32, 347–356.

Moaveni, B., He, X., Conte, J., Restrepo, J., and Panagiotou, M. (2011). "System identification study of a 7-story full-scale building slice tested on the USCD-NEES shake table." *ASCE Journal of Engineering Mechanics*, 137(6), 705–717.

Moaveni, B., Barbosa, A.R., Conte, J.P. and Hemez, F. (2012). "Uncertainty analysis of system identification results obtained for a seven story building slice tested on the UCSD-NEES shake table." *Structural Control and Health Monitoring*, under review.

Mosegaard, K. and Tarantola, A. (1995). "Monte Carlo sampling of solutions to inverse problems." *Journal of Geophysical Research*, 100, 12431–12447.

Mottershead, J. and Friswell, M. (1993). "Model updating in structural dynamics: a survey." *Journal of Sound and Vibration*, 167(2), 347–375.

Muto, M. and Beck, J. (2008). "Bayesian updating and model class selection for hysteretic structural models using stochastic simulation." *Journal of Vibration and Control*, 14(1–2), 7–34.

Panagiotou, M., Restrepo, J., and Conte, J. (2011). "Shake table test of a full-scale 7-story building slice. Phase I: rectangular wall." *ASCE Journal of Structural Engineering*, 137(6), 691–704.

Papadimitriou, C. (2004). "Optimal sensor placement for parametric identification of structural systems." *Journal of Sound and Vibration*, 278, 923–947.

Papadimitriou, C., Beck, J., and Au, S. (2000). "Entropy-based optimal sensor location for structural model updating." *Journal of Vibration and Control*, 6(5), 781–800.

Papadimitriou, C., Beck, J., and Katafygiotis, L. (1997). "Asymptotic expansions for reliability and moments of uncertain systems." *ASCE Journal of Engineering Mechanics*, 123(12), 1219–1229.

Peeters, B. and De Roeck, G. (2001). "Stochastic system identification for operational modal analysis: A review." *ASME Journal of Dynamic Systems, Measurement, and Control*, 123(4), 659–667.

Reynders, E. and De Roeck, G. (2008). "Reference-based combined deterministic-stochastic subspace identification for experimental and operational modal analysis." *Mechanical Systems and Signal Processing*, 22(3), 617–637.

Reynders, E., Pintelon, R., and De Roeck, G. (2008). "Uncertainty bounds on modal parameters obtained from Stochastic Subspace Identification." *Mechanical Systems and Signal Processing*, 22(4), 948–969.

Rytter, A. (1993). "Vibration based inspection of civil engineering structures." Ph.D. thesis, Aalborg University, Aalborg University.

Schevenels, M., Lombaert, G., Degrande, G., and François, S. (2008). "A probabilistic assessment of resolution in the SASW test and its impact on the prediction of ground vibrations." *Geophysical Journal International*, 172(1), 262–275.

Sibilio, E., Ciampoli, M., and Beck, J. (2007). "Structural health monitoring by Bayesian upating." *Proceedings of the ECCOMAS Thematic Conference on Computational Methods in Structural Dynamics and Earthquake Engineering*, Rethymno, Crete, Greece (June).

Sohn, H. and Law, K. (1997). "A Bayesian probabilistic approach for structure damage detection." *Earthquake Engineering and Structural Dynamics*, 26(12), 1259–1281.

Soize, C. (2000). "A nonparametric model of random uncertainties for reduced matrix models in structural dynamics." *Probabilistic Engineering Mechanics*, 15, 277–294.

Soize, C. (2003). "Probabilités et modélisation des incertitudes: éléments de base et concepts fondamentaux (May).

Soize, C. (2008). "Construction of probability distributions in high dimensions using the maximum entropy principle: applications to stochastic processes, random fields and random matrices." *International Journal for Numerical Methods in Engineering*, 75, 1583–1611.

Soize, C. (2010). "Generalized probabilistic approach of uncertainties in computational dynamics using random matrices and polynomial chaos decompositions." *International Journal for Numerical Methods in Engineering*, 81(8), 939–970.

Soize, C. (2011). "Stochastic modeling of uncertainties in computational structural dynamics – recent theoretical advances." *Journal of Sound and Vibration* doi:10.1016/j.jsv.2011.10.010.

Tarantola, A. (2005). *Inverse problem theory and methods for model parameter estimation*. SIAM, Philadelphia, USA.

Teughels, A., Maeck, J., and De Roeck, G. (2002). "Damage assessment by FE model updating using damage functions." *Computers and Structures*, 80(25), 1869–1879.

Vanik, M., Beck, J., and Au, S. (2000). "Bayesian probabilistic approach to structural health monitoring." *ASCE Journal of Engineering Mechanics*, 126(7), 738–745.

Yuen, K.-V. (2010a). *Bayesian methods for structural dynamics and civil engineering*. John Wiley & Sons, Singapore, 1st edition.

Yuen, K.-V. (2010b). “Recent developments of Bayesian model class selection and applications in civil engineering.” *Structural Safety*, 32(5), 338–346.

Yuen, K.-V. and Katafygiotis, L. (2002). “Bayesian modal updating using complete input and incomplete response noisy measurements.” *ASCE Journal of Engineering Mechanics*, 128(3), 340–350.

Yuen, K.-V., Katafygiotis, L., Papadimitriou, C., and Mickleborough, N. (2001). “Optimal sensor placement methodology for identification with unmeasured excitation.” *ASME Journal of Dynamic Systems, Measurement, and Control*, 123(4), 677–686.

List of Tables

TABLE 1: The five damage states and corresponding imposed historical earthquake records.

Damage state	Earthquake record			
	Earthquake	Component	Recorded at	M
S0	None	-	-	-
S1	1971 San Fernando	longitudinal	Van Nuys	6.6
S2	1971 San Fernando	transversal	Van Nuys	6.6
S3	1994 Northridge	longitudinal	Oxnard Blvd.	6.7
S4	1994 Northridge	360 degree	Oxnard Blvd.	6.7

TABLE 2: Experimentally identified natural frequencies and damping ratios for the five damage states.

Damage state	f_{exp} [Hz]			ξ_{exp} [%]		
	Mode 1	Mode 2	Mode 3	Mode 1	Mode 2	Mode 3
S0	1.91	10.51	24.51	2.3	2.4	0.5
S1	1.88	10.21	24.31	2.9	2.7	0.6
S2	1.67	10.16	22.60	1.3	1.4	0.9
S3	1.44	9.23	21.82	2.7	1.3	1.4
S4	1.02	5.67	15.10	1.0	1.7	1.0

TABLE 3: Initial values, MAP estimates obtained through deterministic updating and MCMC, posterior mean values μ, standard deviations σ and coefficients of variation (COV) for S0.

Sub-structure	$\boldsymbol{\theta}^{\text{init}}$	S0 [GPa] $\boldsymbol{\theta}_{\text{opt}}^{\text{MAP}}$	$\boldsymbol{\theta}_{\text{MCMC}}^{\text{MAP}}$	$\mu(\sigma)$	COV [%]
1	24.50	19.71	20.91	21.33 (5.10)	23.9
2	24.50	25.05	24.83	27.41 (8.77)	32.0
3	26.00	28.74	27.87	31.56 (9.86)	31.3
4	26.00	26.52	27.79	28.07 (6.75)	24.0
5	34.80	35.07	36.06	37.23 (9.25)	24.8
6	34.80	36.18	32.56	38.12 (9.19)	24.1
7	30.20	31.96	29.14	33.43 (7.69)	23.0
8	28.90	28.73	31.53	31.42 (7.26)	23.1
9	32.10	31.81	32.67	35.14 (8.33)	23.7
10	33.50	33.61	33.12	36.05 (8.93)	24.8

TABLE 4: MAP-values and coefficients of variation (COV) for the 10 substructure stiffnesses, for all damage states.

Sub-	S0		S1		S2		S3		S4	
structure	MAP [GPa]	COV [%]	MAP [GPa]	COV [%]	MAP [GPa]	COV [%]	MAP [GPa]	COV [%]	MAP [GPa]	COV [%]
1	20.91	23.9	19.56	23.1	12.66	24.4	7.96	22.7	1.16	19.1
2	24.83	32.0	25.92	33.0	25.92	38.3	21.61	40.1	20.53	37.7
3	27.87	31.3	26.17	31.7	23.97	35.6	18.43	40.8	17.80	40.9
4	27.79	24.1	28.36	24.3	30.12	25.0	30.04	25.9	25.81	27.0
5	36.06	24.8	36.06	24.7	37.03	25.4	33.70	25.3	29.94	27.6
6	32.56	24.1	32.36	24.3	31.27	24.6	28.80	24.9	25.82	29.0
7	29.14	23.0	30.35	23.2	29.40	23.4	28.43	24.6	9.68	36.2
8	31.53	23.1	32.68	23.2	35.44	22.5	39.10	24.0	30.18	32.7
9	32.67	23.7	33.06	22.9	33.94	22.7	36.49	24.5	35.07	27.3
10	33.12	24.8	33.01	24.0	36.53	24.3	33.13	25.4	31.18	25.8

List of Figures

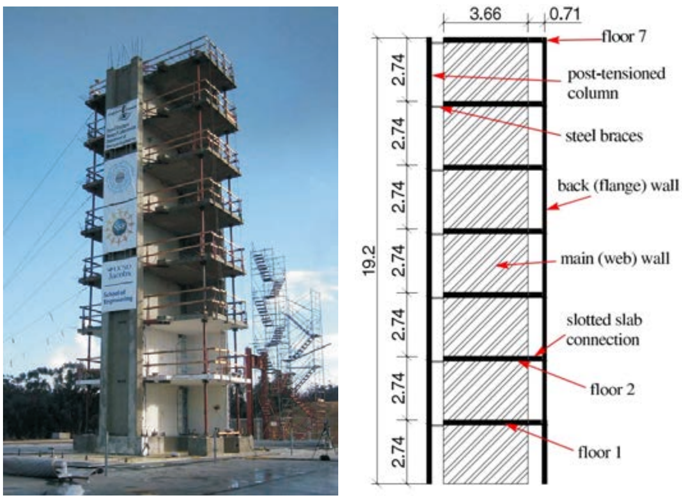

(a) (b)

FIG. 1: (a) Seven-story test structure and (b) elevation view.

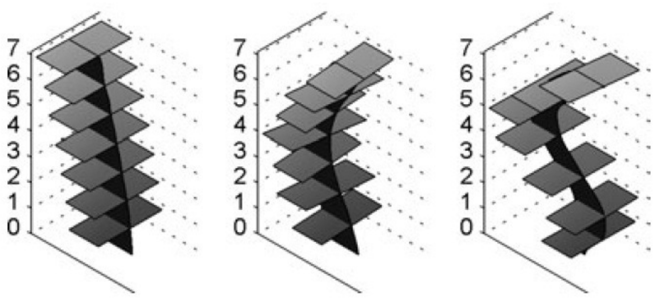

FIG. 2: First three longitudinal mode shapes obtained at damage state S0.

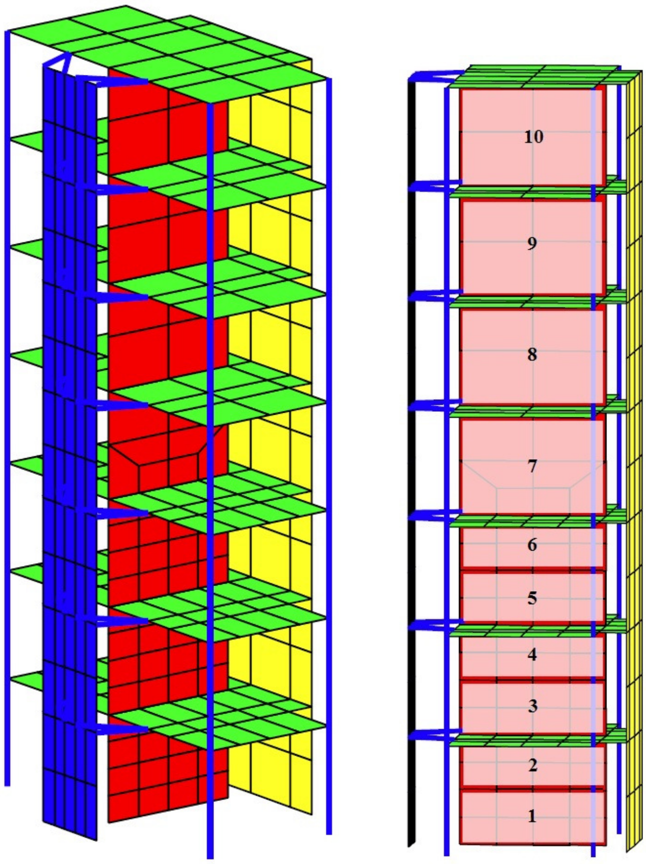

(a) (b)

FIG. 3: (a) FE model of the seven-story test structure and (b) definition of the substructures along the main wall.

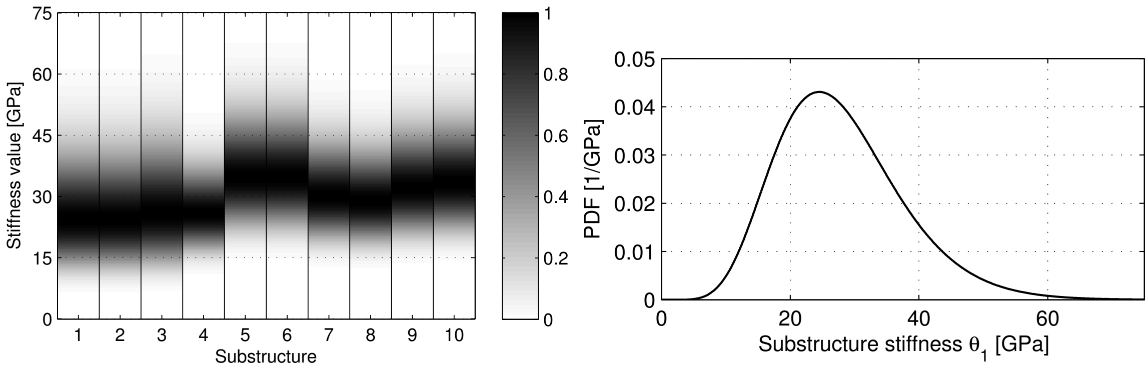

(a) (b)

FIG. 4: (a) Contour plot of the normalized marginal prior PDFs and (b) marginal prior PDF for substructure 1, for damage state S0.

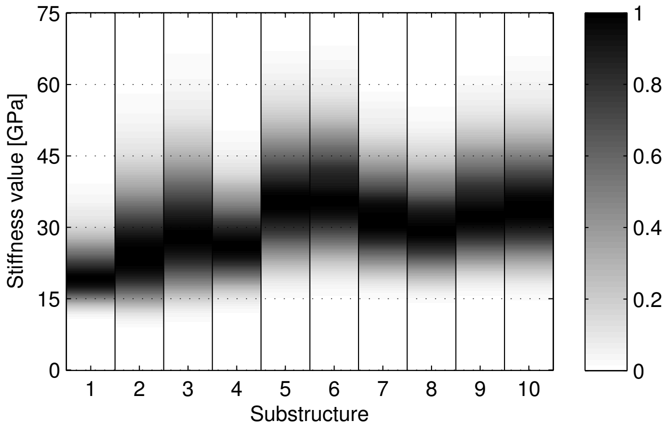

FIG. 5: Contour plot of the normalized marginal posterior PDFs for all substructures, for damage state S0.

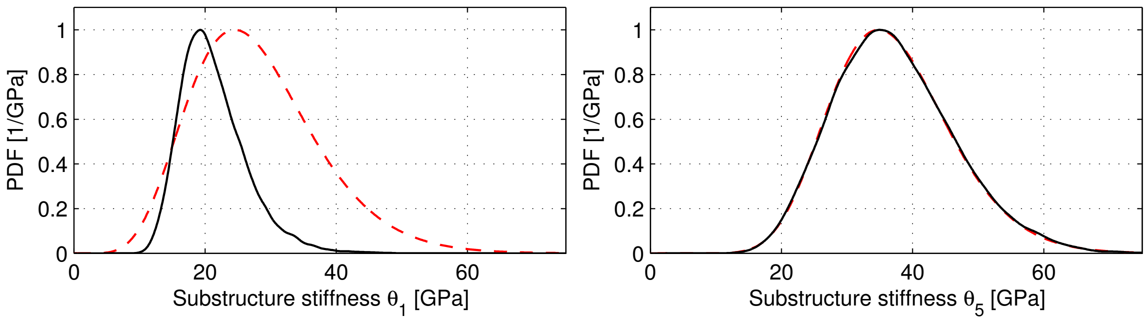

(a) (b)

FIG. 6: Normalized marginal prior PDF (dashed line) and posterior PDF (solid line) for (a) substructure 1 and (b) substructure 5, for damage state S0.

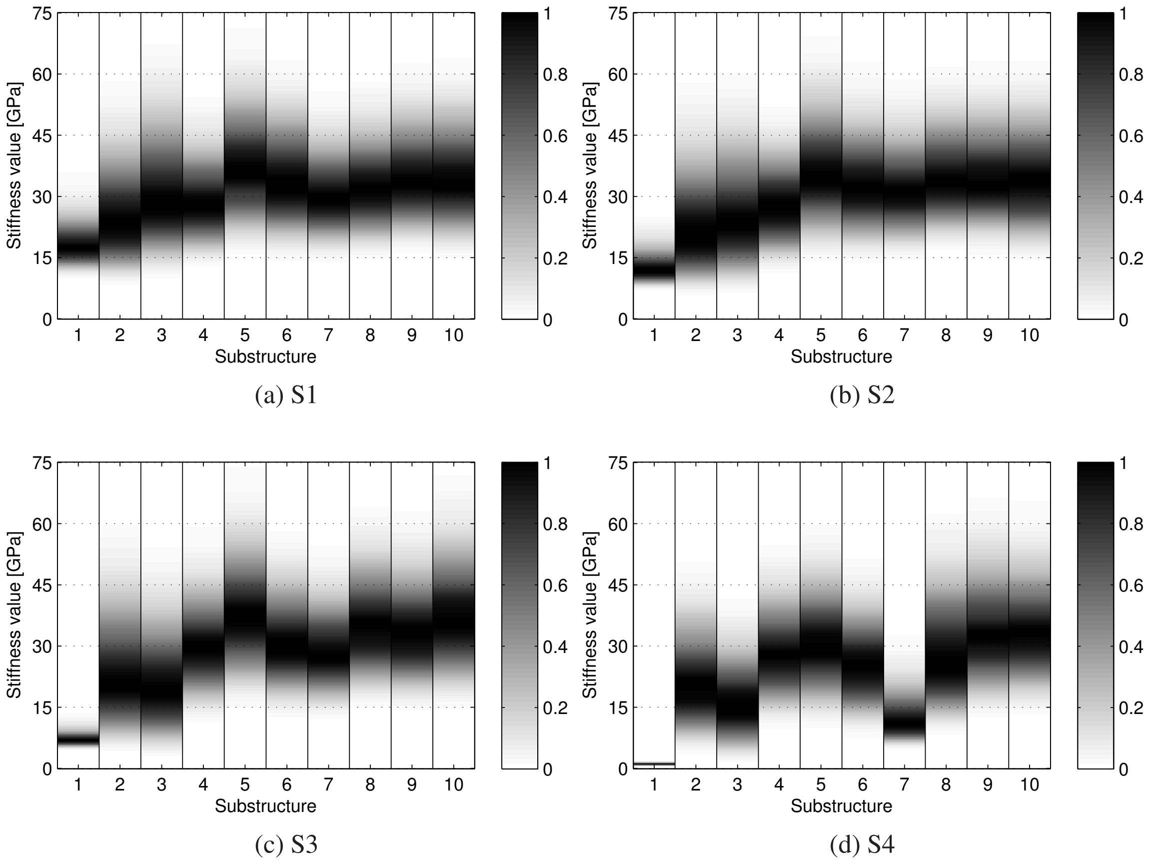

FIG. 7: Contour plot of the normalized marginal posterior PDFs for all substructures, for damage states S1 to S4.

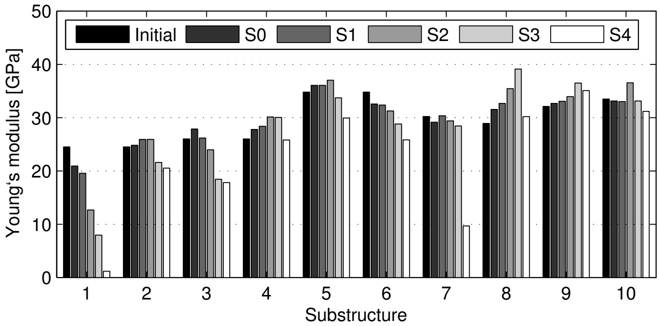

FIG. 8: Initial stiffness values $\boldsymbol{\theta}^{\text{init}}$ and MAP stiffness values for all damage states.

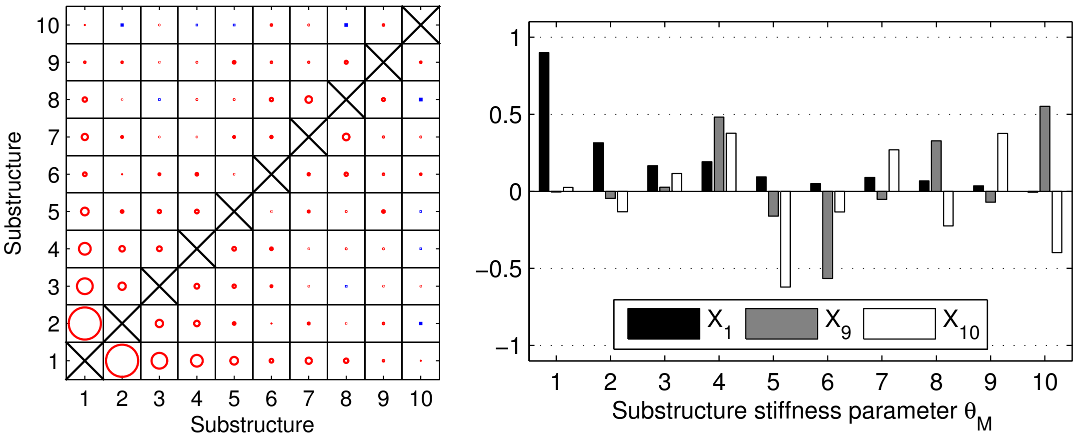

(a) (b)

FIG. 9: (a) Visualization of posterior correlation coefficient matrix where the relative size of the symbols represents the value of the negative (○) and positive (□) correlation coefficients, and (b) the best (X_1) and two worst (X_9 and X_{10}) resolved parameter combinations, for damage state S0.

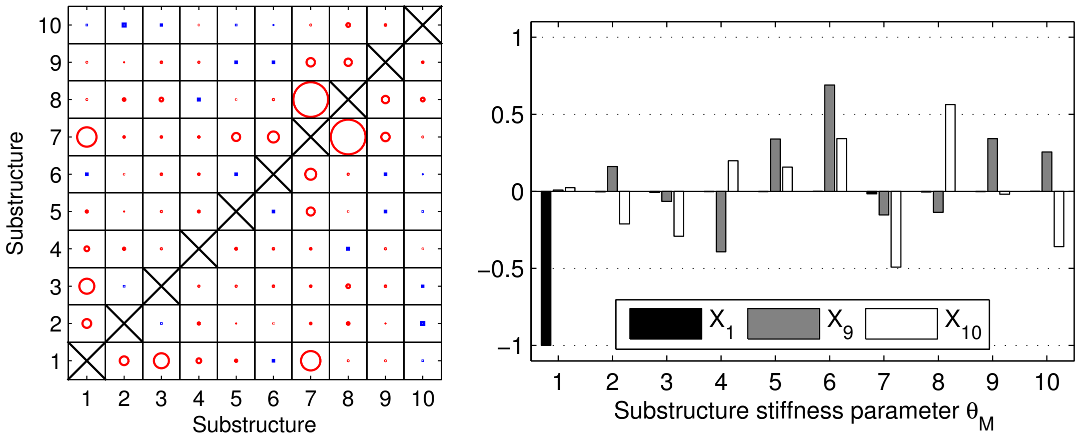

(a) (b)

FIG. 10: (a) Visualization of posterior correlation coefficient matrix where the relative size of the symbols represents the value of the negative (○) and positive (□) correlation coefficients and (b) the best (X_1) and two worst (X_9 and X_{10}) resolved parameter combinations, for damage state S4.